JPhys Materials

ACCEPTED MANUSCRIPT • OPEN ACCESS

Belousov-Zhabotinsky reaction in liquid marbles

To cite this article before publication: Claire Fullarton *et al* 2018 *J. Phys. Mater.* in press https://doi.org/10.1088/2515-7639/aaed4c

Belousov-Zhabotinsky reaction in liquid marbles

Claire Fullarton[1], Thomas C. Draper[1], Neil Phillips[1],
Ben P. J. de Lacy Costello[1,2], and Andrew Adamatzky*[1]

[1]Unconventional Computing Laboratory, University of the West of England, Bristol, UK
[2]Institute of Biosensing Technology, Centre for Research in Biosciences, University of the West of England, Bristol BS16 1QY, UK

Abstract

In Belousov–Zhabotinsky (BZ) type reactions, chemical oxidation waves can be exploited to produce reaction-diffusion processors. This paper reports on a new method of encapsulating BZ solution in a powder coating of either polyethylene (PE) or polytetrafluoroethylene (PTFE), to produce BZ liquid marbles (LMs). BZ LMs have solid-liquid interfaces compared to previously reported encapsulation systems, BZ emulsions and BZ vesicles. Oscillation studies on individual LMs established PE-coated LMs were easier to prepare and more robust than PTFE-coated LMs. Therefore, this coating was used to study BZ LMs positioned in ordered and disordered arrays. Sporadic transfer of excitation waves was observed between LMs in close proximity to each other. These results lay the foundations for future studies on information transmission and processing arrays of BZ LMs. Future work aims to elucidate the effect of other physical stimuli on the dynamics of chemical excitation waves within these systems.

Keywords: Liquid marbles, Belousov-Zhabotinsky (BZ) reaction, chemical excitation wave propagation

Introduction

Understanding the dynamics of reaction-diffusion (RD) processes and their resultant systems has been of interest to researchers over the past few decades. These systems have been employed to prepare nano-structures, micro-structures and active materials via self-assembly and self-organisation processes [1–4]. More focus is now needed on understanding the spatiotemporal dynamics of these systems at different scales [5–8]. Belousov–Zhabotinsky (BZ) type reactions are well established RD systems, which have been shown to generate 3D Turing patterns, phase waves, trigger waves and scroll waves, via chemical excitation mechanisms, when geometrically confined [9–12]. BZ reactions involve the oxidation of an organic substrate, typically malonic acid, by bromate ions in the presence of an acid, typically sulphuric acid, and a one electron transfer metal ion redox catalyst, e.g. ferroin [1, 13–15].

These reactions have proved to be potential media for developing future and emergent computing devices based on the interaction of chemical wave-fragments. A substantial number of theoretical studies and experimental prototypes of computing devices have been implemented using this media; image processors and memory devices [15–17], logical gates implemented in geometrically constrained BZ media [18, 19], approximation of the shortest path of excitation waves [20–22], information coding using the frequency of oscillations [23], onboard controllers for robots [24–26], chemical diodes [27], neuromorphic architectures [28–34] and associated memory [35, 36], wave-based counters [37] and other information processors [32, 38–40].

* *Corresponding author. Email: Andrew.Adamatzky@uwe.ac.uk*

To provide insights into these processes and the use of BZ media for the applications above, previous studies ultilised the BZ reaction in spatially confining media such as thin hydrogel films [41], small droplets in microfluidic devices [32, 42–52], vesicles [53–57], emulsions [58], BZ-AOT emulsions [9–11, 17, 59–64], cation exchange resins [65–71] and 3D printed structures [42, 72, 73].

Liquid marbles (LMs), first reported by Aussillous and Quéré [74], provide a means of moving droplets across a surface without wetting the underlying substrate. This avoids surface contamination problems and allows fast displacement and easy manoeuvrability of the droplets. To prepare LMs, droplets of liquid are encapsulated in a powder coating by rolling the droplets on a powder bed or via an electrostatic method [74, 75]. The powder coatings are typically hydrophobic powders such as polyethylene (PE) or polytetrafluoroethylene (PTFE), however hydrophilic powders have also been reported e.g. carbon black [76]. It is possible to use hydrophilic powders to prepare LMs due to surface roughness induced hydrophobicity [77]. In the context of using LMs as a method for encapsulating the BZ reaction, they avoid the use of microfluidic systems and allow BZ media to be probed in a solid–liquid system rather than in a liquid–liquid system e.g. BZ media in vesicles and emulsions. Properties of LMs can be tailored for a variety of applications by altering the encapsulated liquid and / or the powder coating [78–83]. This tailoring can enable LMs to be manipulated using electric and magnetic fields, as well as being able to be mechanically manipulated [84]. Therefore, LMs can be forced to merge together, through collisions or field effects, split into daughter LMs (if there is a sufficient amount of coating on the daughter LMs to not wet the underlying substrate), opened, closed, easily modified in terms of adding and removing liquid from a pre-made LM, as well as being permeable to gas, due to the powder coating [85–91]. The preparation of complex LMs reported in the literature, proves the resilience of LM systems and their ability to transport a range of chemical cargoes. LMs have been reported to be prepared from aqueous media, organic media, ionic liquids and biological media [74, 83, 92–98]. The encapsulated liquid and / or the powder coating can play mediating roles in chemical reactions [99, 100].

This paper reports on the preparation of acidic LMs using BZ solution as the liquid encapsulated in a polymer powder coating of either PE or PTFE. The BZ solution inside the LM was optically monitored to observe whether pattern formation occurred and if chemical excitation waves propagated inside the LM. Arrays of BZ solution LMs prepared assessed whether the transmission of chemical excitation waves occurred between LMs in close proximity, referred to throughout as wave transfers, as well as observing the collective behaviour of the oscillating system. These experiments lay the foundations for developing unconventional computing devices using LMs as a means of encapsulating BZ solution, in a system which can be reconfigured into various different architectures.

Experimental

The ferroin-catalysed / malonic acid BZ reaction studied was prepared using the method reported by Field [101], omitting the surfactant Triton X. 18 M Sulphuric acid H_2SO_4 (Fischer Scientific, CAS 7664-93-9), sodium bromate $NaBrO_3$ (Sigma Aldrich, CAS 7789-38-0), malonic acid $CH_2(COOH)_2$ (Sigma Aldrich, CAS 141-82-2), sodium bromide NaBr (Sigma Aldrich, CAS 7647-15-6) and 0.025 M tris-(1,10-phenanthroline) iron(II) sulphate (ferroin indicator, Sigma Aldrich - Honeywell Fluka, CAS 14634-91-4) were used as received. Coatings for LMs, ultra high density polyethylene (PE) (Sigma Aldrich, CAS 9002-88-4, Product Code 1002018483) and polytetrafluoroethylene (PTFE) (Alfa Aesar, CAS 9002-84-0, Product Code 44184) were used as received, with particle sizes 100 μm and 6 μm–10 μm respectively.

H_2SO_4 (2 ml) was added to deionised water (67 ml), to produce 0.5 M H_2SO_4, $NaBrO_3$ (5 g) was added to yield 70 ml stock solution, containing 0.48 M $NaBrO_3$. Stock solutions of 1 M malonic acid and 1 M NaBr were prepared by dissolving 1 g in 10 ml of deionised water.

In a 50 ml beaker, 0.5 ml of 1 M malonic acid was added to 3 ml of the acidic $NaBrO_3$ solution.

0.25 ml of 1 M NaBr was then added to the beaker, which produced bromine. The reaction was left, until a clear colourless solution remained (ca. 5 min) before adding 0.5 ml of 0.025 M ferroin indicator to the beaker.

BZ LMs were prepared by pipetting droplets of BZ reaction mixture (50 and 100 μl), which was already oscillating, on to a powder bed of either polyethylene (PE) or polytetrafluoroethylene (PTFE) in a weighing boat, releasing the droplet ca. 5 mm from the top of the powder bed. The BZ droplet was rolled on the powder bed for 10 s to produce a LM. The coatings of the prepared LMs consisted of multi-layers of particles, rather than a single layer. The single BZ LMs were then transferred on to a cool white LED housed in a black plastic box (single 5 mm diameter cool white LED 5000–8300 K, powered by a standard 9 V battery) to highlight the oscillating reaction inside the LM and enable the observation of travelling wave-fronts through the LM coating. Disordered arrays of LMs were prepared by transferring the pre-made LMs into a Petri dish. Ordered LM arrays were prepared by rolling LMs onto a 4 x 4 plastic polypropylene template comprised of wells with a diameter of ca. 2 mm and a depth of ca. 1 mm. Both BZ arrays were then illuminated by using an LED light underneath the Petri dish. The BZ reaction in LMs was recorded using an otoscope-style USB microscope (MixMart, China).

PTFE LMs were not as robust as PE LMs, sometimes bursting upon transfer, which therefore meant they took longer to position under the microscope. The PTFE LMs took ca. 20 min to prepare and position after the reaction was initiated. In contrast, PE LMs took ca. 5 min which meant the oscillating reaction continued for longer once encapsulated within the PE powder coating.

Results

Initially, to investigate the feasibility of preparing stable LMs using the acidic BZ media, powder coatings of PE and PTFE were studied. PE and PTFE have previously been demonstrated as suitable coatings for LMs. They are relatively inert to acidic solutions, provide a comparison between LM coating particle sizes and appear translucent when illuminated with an LED [102]. The latter meant it was possible to observe the oxidation waves through both PE and PTFE coatings. The difference in particle size of the coatings, varied the particle spacing on the surface of the LM, which therefore varied, to different degrees, the observations of the oscillating BZ solution within the LM. Studies focused initially on observing the colour changes and oxidation waves of the BZ media in single LMs. The single BZ LM experiments proved which out of the two coatings selected would be a viable coating to encapsulate the BZ media in. After observing the behaviour of single LMs, the behaviour of oxidation waves in disordered and ordered arrays of PE-coated LMs was observed. Small impacts and collisions caused both PE BZ LMs and PTFE BZ LMs to coalesce or burst relatively easily. Due to the heterogeneous nature of the LM surface, LMs with the same encapsulated liquids and coatings can have varying properties. This means only sometimes they burst or coalesce with other LMs. Failures of LMs and robustness studies during impact have recently been investigated and shown to vary with particle coating and size of the LMs [85, 102, 103]. PE-coated LMs were easier to roll into position over either the LED to record a single LM or position into disordered and ordered arrays. The larger size particles of PE were found to produce more stable LMs which were robust enough to survive being manoeuvred across a surface and transported between different surfaces. This is in contrast to some previous work reported in the literature [104, 105], which reports that smaller particles lead to more stable LMs. This would be the case if LMs remained static after preparation. However in practice, the transfer of the LMs after preparation shows larger particles produce more robust LMs, fine particle LMs tend to burst upon transfer onto different surfaces. The interactions between particles in the coatings of LMs, allow the particles to arrange themselves on the surface of the liquid droplet. It has been suggested that capillary forces act on the particle in the coating, with the type of powder determining whether these forces are attractive or repulsive between particles [81, 106].

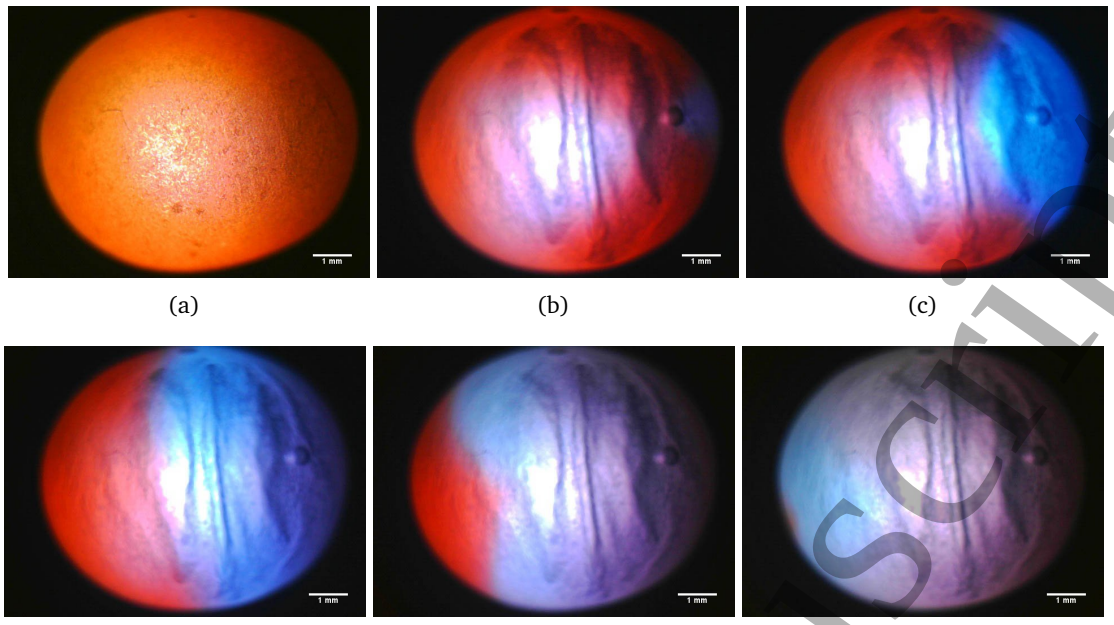

Figure 1: A single 50 μl PTFE-coated BZ LM showing the LM at the start of the recording (a) and showing the first oxidation wave observed (b–f) which took 25 s to travel from one side of the viewable area of the LM to the other. The corresponding video can be found in the SI (S1). Scale: 5 mm on image equivalent to 1 mm. LM horizontal diameter 8.1 mm. Between images (a) and (b) the coating of the LM changed from smooth to wrinkled, referred to as a buckled coating, and a gas bubble appeared on the right hand side of the LM ca. 0.5 mm in diameter.

The concentration of BZ solution used to make the LMs, exhibited oscillating behaviour. When the BZ solution prepared was left unstirred in a thin film in a Petri dish, pattern formation in the form of trigger waves occurred in the BZ solution. As the reaction was in an excitable phase these spontaneous trigger waves degenerated into spiral waves as the reaction proceeded. Spiral waves occurred due to the spontaneous breaking of circular trigger waves by gas bubbles. The BZ reaction involves three major reactions; firstly the reduction of bromide ions by bromate ions, secondly the autocatalytic species, bromous acid ($HBrO_2$), oxidises the reduced form of the catalyst ferroin (Fe(II)) to ferriin (Fe(III)), and thirdly, when the Fe(III) reaches a high enough concentration, this initiates the reaction of the organic substrate, in this case, malonic acid, and its brominated derivative, bromomalonic acid, to yield the reduced catalyst, ferroin and bromide ions (reaction inhibitor), which initiates the first reaction again. The changes in oxidation state of the catalyst (Fe(II) / Fe(III)), result in a colour change from red to blue. The intermediate $HBrO_2$ is the reaction activator (autocatalytic species), the diffusion of which enables the propagation of chemical excitation waves through the media.

Figure 1 shows the propagation of the first travelling wave observed in a single 50 μl PTFE-coated BZ LM. The LMs reported in this paper sometimes appear ellipsoid. This is described in the literature as quasi-spherical for small LMs. The larger the volume of the LM, the more ellipsoid (puddle-like) the shape [81]. Also, the shape can be affected by rolling the LM into position. The periods of oscillation, the times recorded between two waves passing through the same point through the LM, were found to decrease as the reaction proceeded. Periods were recorded for single LMs, by observing the waves passing through the vertical diameter of the LM images. These are reported for the single LMs in the SI. Ten travelling waves were visible during the course of the reaction. At the start of the experiment, it appeared there could be some centralised oscillations or a spot of oxidised catalyst in the centre of the viewable LM,

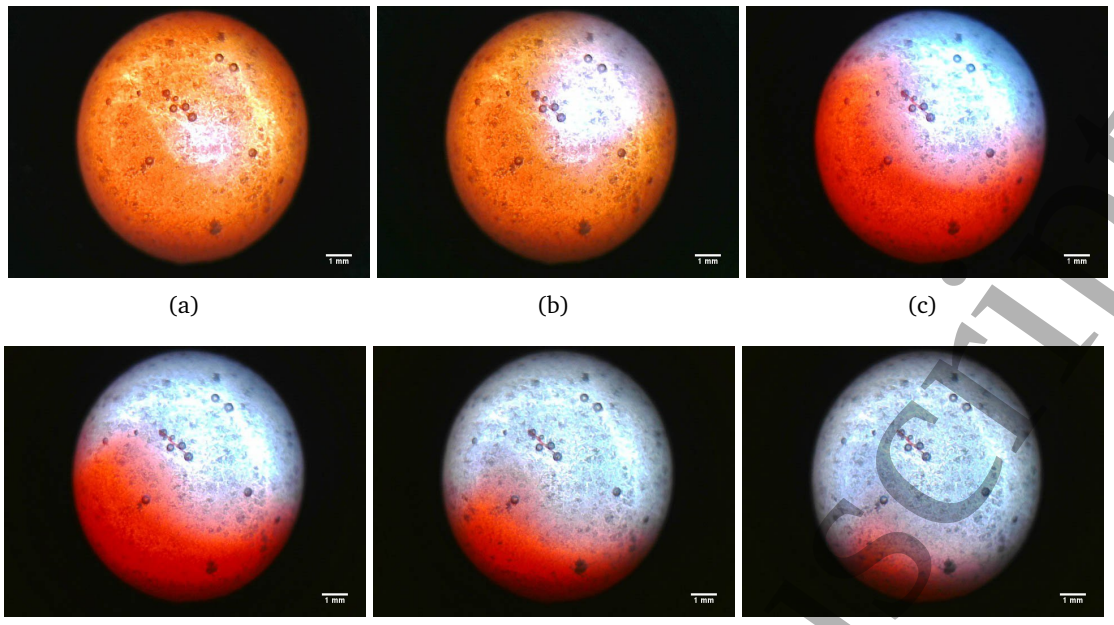

Figure 2: A single 100 μl PTFE-coated BZ LM showing the only wave observed (a–f) which took 35 s to travel from one side of the viewable area of the LM to the other. The corresponding video can be found in the SI (S2). Scale: 3 mm on image equivalent to 1 mm. LM horizontal diameter 9 mm. Small gas bubbles ca. 0.3 mm in diameter can be seen in all images.

shown in Fig. 1b and SI video (S1). These oscillations could be 3D scroll waves propagating within the LM however, they are not clearly visible. There was an induction period of ca. 11 min observed once the BZ solution had been encapsulated in the PTFE. After the induction period, travelling waves propagated from right to left across the LM, shown in Fig. 1b–f. The LM started buckling after only ca. 2 min after LM positioning. Buckling refers to the collapsing of the LM coating. This has been reported to originate from the top centre of LMs, due to the evaporative loss of liquid from the entire LM followed by the re-arrangement of the remaining liquid under gravity. This subsequently leaves a void at the upper surface which results in the buckling of the powder wall of the LM [107]. In Fig. 1e it appears the travelling wave splits into two wave-fronts, potentially arising from the buckling of the LM coating. Some gas evolution can be observed, shown by the trapped bubble ca. 0.5 mm in diameter, shown in Fig. 1b–f. The catalyst remained in the oxidised state (ferriin) inside the LM after ca. 25 min. The time taken to prepare and position the LMs reduced the length of time the BZ reaction oscillated inside the LMs. It could be possible that O_2 infiltration through the coating reduced the lifetime of oscillations in the encapsulated solution [108]. LMs are permeable to gas and their use as gas sensors has been reported in the literature [96, 109].

Figure 2 shows the propagation of the only travelling wave observed in a single 100 μl PTFE-coated BZ LM. Only one oscillation was observed, due to taking significantly longer to prepare a viable PTFE-coated BZ LM to record. It took ca. 20 min to prepare and position the LM over the top of the LED prior to recording the system. Therefore, due to this and the fast onset of buckling of the coating, no further experiments were performed on PTFE-coated BZ LMs.

Figure 3 shows the first and second travelling waves observed in a single 50 μl PE-coated BZ LM. Periods of oscillation decreased throughout the course of the reaction. These are reported in the SI. 57 single travelling waves were visible, which moved across the LM from top to bottom. After ca. 2 min small random movements of the LM was observed. However, it was hard to judge whether these movements could be due to variations in inter-facial tension due to the travelling

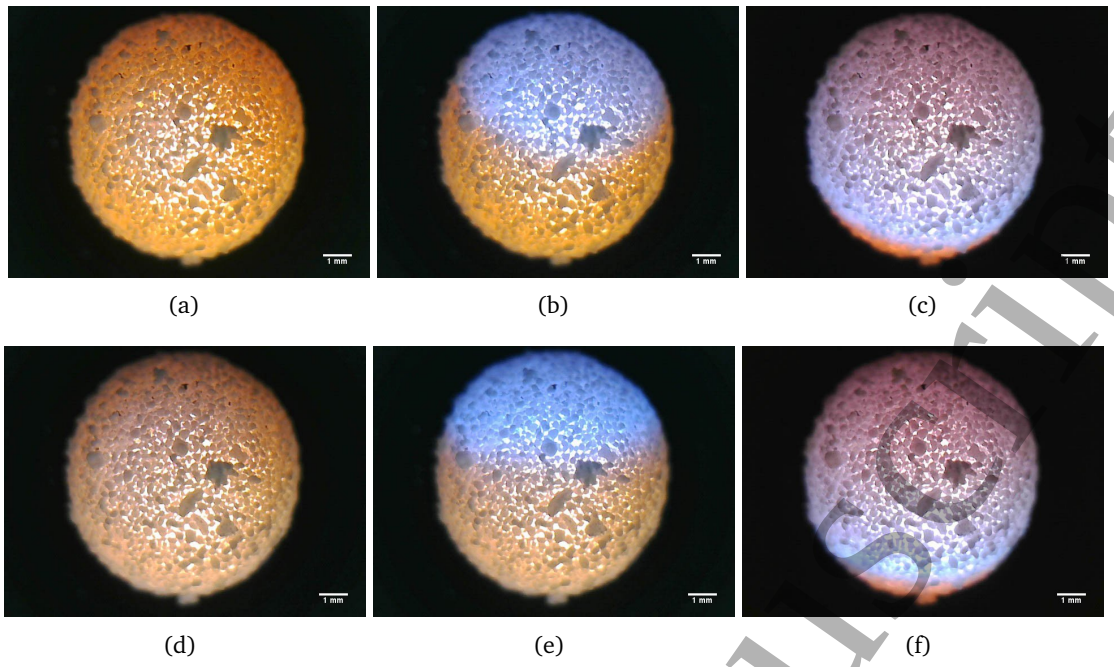

Figure 3: A single 50 μl PE-coated BZ LM showing the first oxidation wave (a–c) which took 25 s to travel from one side of the viewable LM area to the other and the second oxidation wave (d–f) which took 26 s to travel across the LM area. The corresponding video can be found in the SI (S3). Scale: 4 mm on image equivalent to 1 mm. LM horizontal diameter 8.1 mm. The grey particles observed on the surface of the LM are PE powder particles which have formed multi-layers on the surface.

waves, previously observed in BZ droplets in oil [43, 46, 47] or simply the movement of the powder coating due to evaporation of the encapsulated BZ solution and gas evolution. Buckling of the 50 μl PE-coated BZ LM was observed after ca. 18 min. Some gas evolution was observed under the coating after ca. 34 min. This gas could be CO_2 and /or CO. It has been reported that CO as well as CO_2 can be evolved from the ferroin catalysed BZ reaction [110]. Travelling waves appeared not to be affected as most had been observed by the time gas evolution had occurred. Multiple oscillations occurred after ca. 36 min, at which time significant buckling of the LM had occurred. Full oxidation of the ferroin to ferriin had occurred within the LM after ca. 55 min.

In a repeat experiment, 32 single travelling waves were visible, slightly less than the previous 50 μl LM, attributed to the preparation and setup time of the LM underneath the camera. The travelling waves in this LM were observed to move across the LM from right to left. Buckling was observed after ca. 19 min, the same as the previous 50 μl LM. After ca. 39 min again some gas evolution occurred. The travelling waves were not easy to distinguish and multiple oscillations started occurring after ca. 45 min. Full oxidation of the ferroin to ferriin had occurred within the LM after ca. 49 min. After this length of time gas bubbles ca. 0.5 mm in diameter could be observed trapped under the buckled coating of the LM.

Figure 4 shows the travelling waves in a single 100 μl PE-coated BZ LM. Six single travelling waves were visible (at 1897 s, three waves were observed at one time, shown in Fig. 4j–l), travelling from right to left across the LM. The three travelling wave observed may actually be turbulence of one wave-front, giving the appearance of three waves. Periods of oscillation are reported in the SI. Gas evolution occurred after ca. 25 min, slightly earlier than observed for 50 μl LMs. Significant buckling of the LM occurred after ca. 30 min. Full oxidation of the ferroin to ferriin has occurred after ca. 42 min.

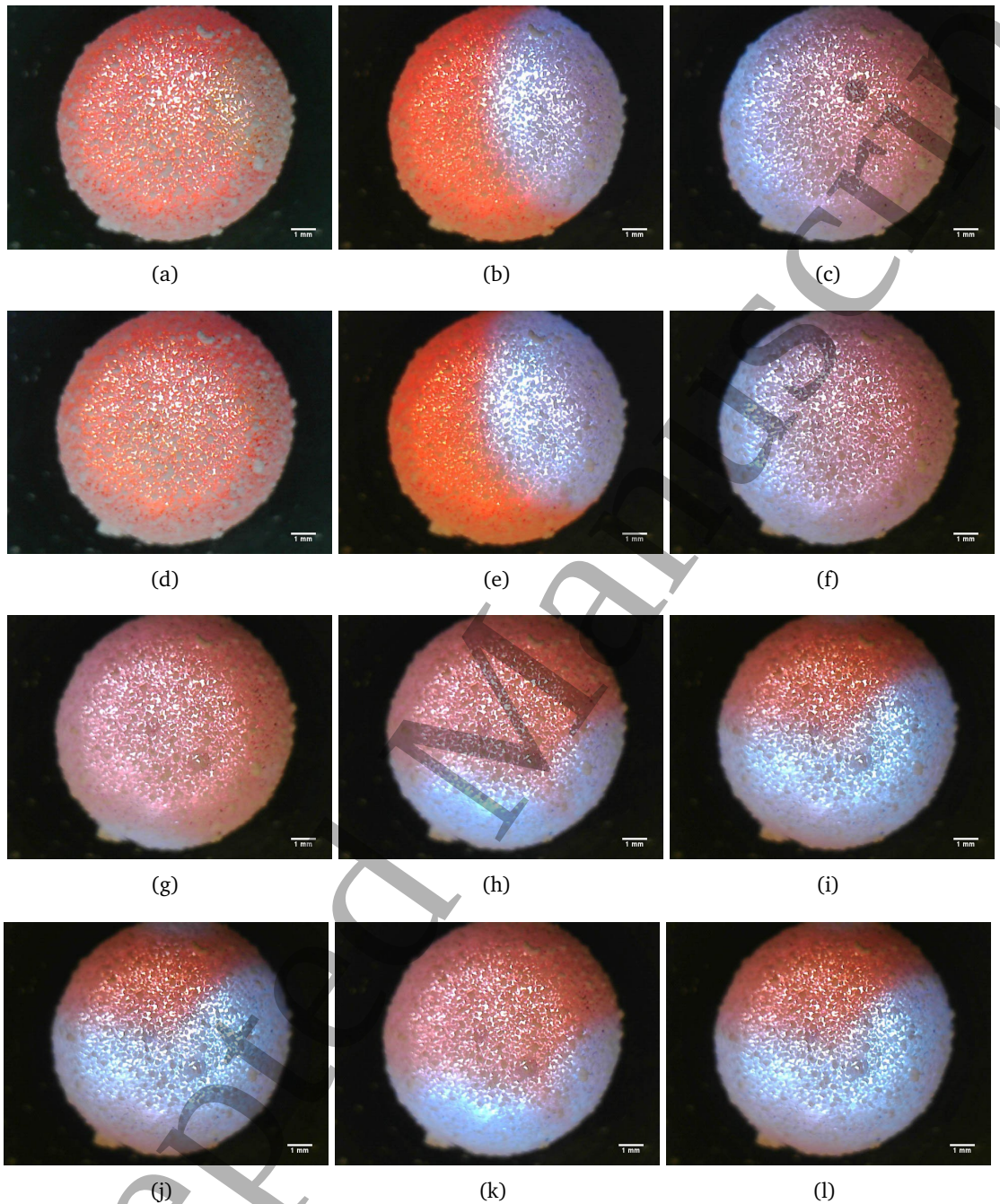

Figure 4: A single 100 μl PE-coated BZ LM coated showing three oxidation wave observed, which took (a–c) 35 s, (d–f) 41 s and (g–l) 33 s to travel across the viewable area of the LM. The corresponding video can be found in the SI (S4). Scale: 3 mm on image equivalent to 1 mm. LM horizontal diameter 9.2 mm.

In a repeat experiment, six single travelling waves were visible, propagating from the bottom to the top of the LM. After ca. 19 min buckling of the 100 μl PE-coated BZ LM was observed. Gas evolution occurred after ca. 25 min, the same as the previous 100 μl single BZ LM analysed. Multiple oscillations occurred after ca. 21 min. Full oxidation of the ferroin to ferriin had occurred within the LM after ca. 42 min. The smaller volume single LMs exhibited more visible oscillations than the larger volume LMs.

It was noted in all LMs prepared, the wave-fronts can be seen to deform as they move across the surface of the LMs. This could be due to physical defects in the surface or there could be hydrodynamic convection caused by concentration dependant surface tension changes around the travelling wave-front [111].

Disordered and ordered arrays of PE-coated BZ LMs were prepared to observe whether transfers of oxidation waves occurred between LMs in close proximity and to report propagation pathways within these different arrays. There was a delay of ca. 5 min when arranging the LMs in the arrays as the LMs were prepared sequentially. However, no correlation between the oscillations in the LMs was observed due to this.

PE-coated BZ LMs for the various arrays were prepared using 50 μl and 100 μl droplets of already oscillating BZ media. For disordered arrays of BZ LMs, a number of LMs of the same volume were rolled into a Petri dish. For the 50 μl and 100 μl BZ LM disordered arrays, the number of LMs used was 14 and 15 respectively. Unfortunately it proved difficult to completely fill the Petri dish, due to stability of the LMs.

To discuss the transfer of waves and propagation pathways, BZ LMs in the disordered arrays were numbered, shown in Fig. 5a for 50 μl and Fig. 5b for 100 μl disordered arrays respectively. 84 individual oscillations were observed in the 50 μl disordered array, Fig. 5a, with 14 of these waves resulting in transfer from one LM to another. Therefore, 17% of oscillations resulted in transfers from one LM to another. All the LMs in the 50 μl disordered array oscillated, LM4 oscillated the most with ten visible wave-fronts, whilst LM3 oscillated the least with four visible wave-fronts. The number of individual oscillations each LM exhibited are reported in Fig. 5a. Out of the 14 waves observed to transfer, two of these waves from two different LMs appeared to result in transfer to a single LM. The longest propagation pathway observed occurs between LM2 – LM4 – LM5 occurring from the third and fourth wave transfers.

For the 100 μl disordered array, 15 LMs were used, shown in Fig. 5b. 153 oscillations were observed, 31 of which resulted in transfers from one LM to another. Therefore, 20% of oscillations resulted in transfers from one LM to another, similar to the percentage observed for the 50 μl disordered array. The number of individual oscillations each LM exhibited are reported in Fig. 5b. The video for the BZ 100 μl disordered array can be found in the SI. The longest propagation pathway observed occurs between three LMs in the 100 μl disordered array.

As can be seen from 50 μl disordered array transfer videos in the SI and the first transfer from the 50 μl disordered array shown as an example in Fig. 6, the direction of oxidation wave transfer between LMs demonstrates that excitation passes through the LM disordered array rather than being a result of spontaneous self-oscillation of the media inside a single LM. Similar wave transfers have been previously observed in BZ vesicles [112] and catalyst loaded particles [113].

Ordered arrays of 50 μl BZ LMs were prepared by using a polypropylene template to position the LMs in a 4×4 arrangement. This allowed more control over the number of contacts each LM had with adjacent LMs. Figure 7 shows a 16 LM ordered array, in which 264 oscillations were observed. The catalyst in all the LMs in the array remained in the oxidised state after ca. 1 h 20 min. Fewer transfers occurred in the ordered array in comparison to the disordered array, with only six inter-marble transfers occurring, meaning only 2% of oscillations transferred to an adjacent LM. The longest pathway observed involved three LMs, occurring during the first and second wave transfers. This pathway is shown by the white arrows in Figure 7. In another 4×4 ordered array, 182 oscillations were observed. The catalyst remained in an oxidised state

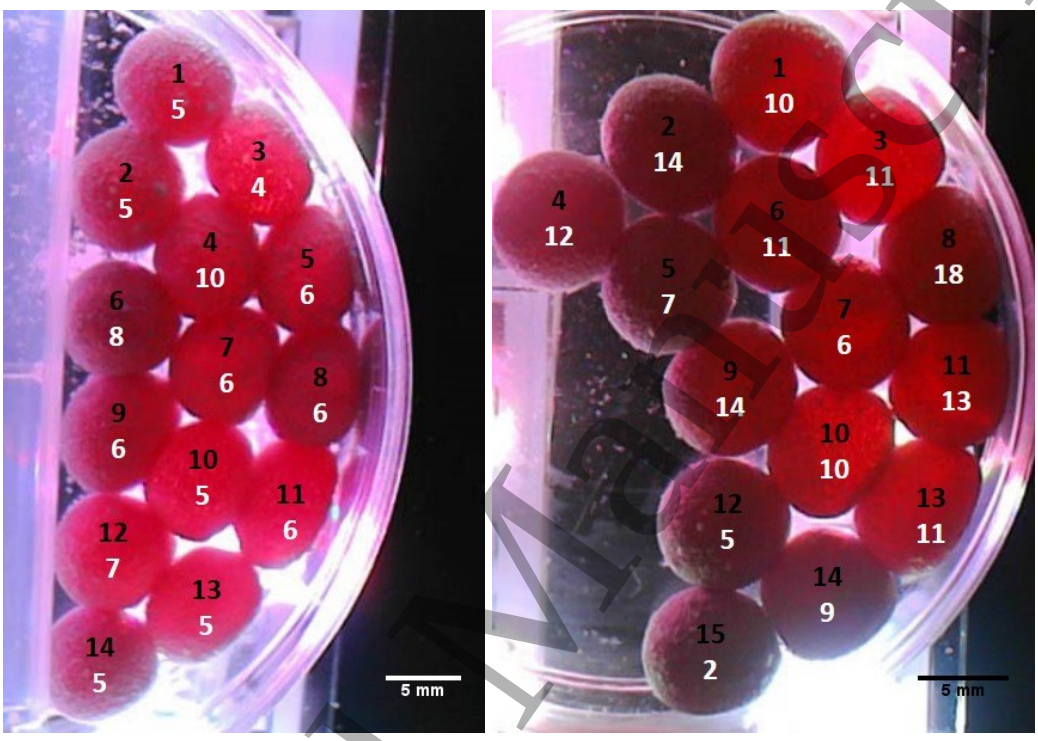

(a) (b)

Figure 5: Disordered arrays of BZ LMs (a) 50 μl PE-coated BZ LM disordered array – top numbers (in black) refer to the numbers assigned to the LMs in the array, bottom numbers (in white) refer to the number of individual oscillations observed in each LM. The corresponding video can be found in the SI (S5). Scale: 10 mm on image equivalent to 5 mm. LM horizontal diameters ca. 8 mm. (b) 100 μl PE-coated BZ LM disordered array – top numbers (in black) refer to the number assigned to the LMs in the array, bottom numbers (in white) refer to the number of individual oscillations observed in each LM. The corresponding video can be found in the SI (S6). Scale: 11 mm on image equivalent to 5 mm. LM horizontal diameters ca. 9 mm.

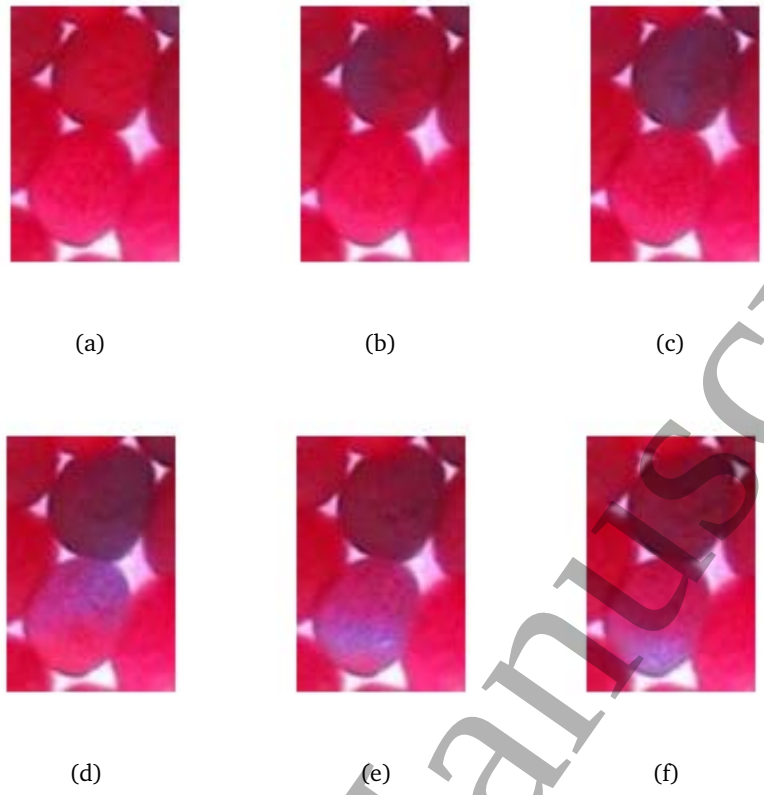

Figure 6: The first wave transfer between two LMs observed in the 50 μl PE-coated BZ LM disordered array, transferring from LM7 to LM10. Scale: 1.625 mm on image equivalent to 1 mm. LM horizontal diameters ca. 8 mm.

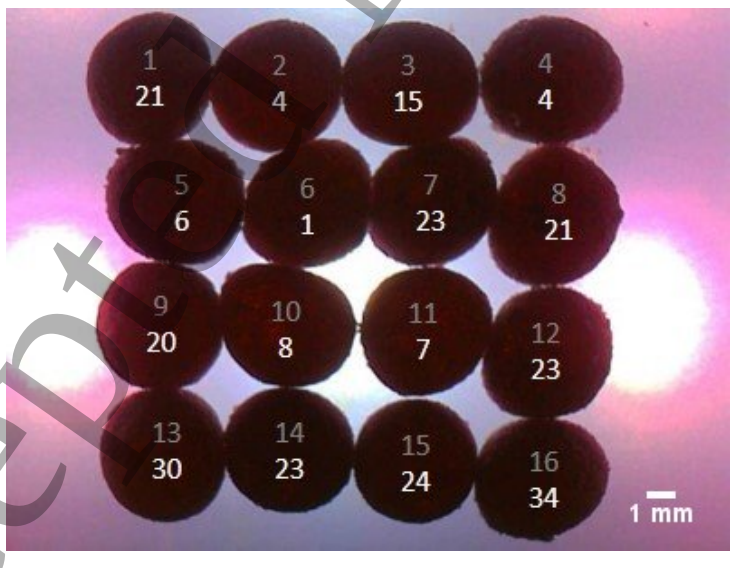

Figure 7: 50 μl PE-coated BZ LM ordered array – top numbers (in grey) refer to the numbers assigned to the LMs in the array, bottom numbers (in white) refer to the number of individual oscillations observed in each LM. The corresponding video can be found in the SI (S7). Scale: 4 mm on image equivalent to 1 mm. LM horizontal diameters ca. 7.5 mm. Arrows in white show the longest wave transfer pathways observed in the array.

in all the LMs in this array after ca. 1 h.

It is envisaged that transmission of chemical excitation waves occurred through the BZ LM array, either through gaseous Br_2 and bromide species transfers between the LMs or possibly liquid–liquid communication through contacts between LMs. The latter occurring due to imperfections on the LM particle coating. It is well known that most liquid marbles possess voids in their surface structure due to incomplete surface coverage [102].

Discussion

The BZ LM array experiments reported above show that it is feasible to observe oxidation waves through the coating of the LMs and observe transfers of these waves between adjacent LMs. It should be possible to control wave transfers by adjusting the chemistry of the encapsulated BZ system. This could be by using a different organic substrate, using a light sensitive catalyst, or by initiating and inhibiting the reaction to obtain controlled wave transfer. It is envisaged that through this controlled wave transfer and varying the arrangement of LMs in arrays, propagation pathways can be controlled and lengthened [114]. This will allow the development of more complex computing devices using BZ LMs, in addition to observing the natural behaviour of the oscillating liquid media encapsulated in a powder coating, rather than in a liquid–liquid droplet system. The ability to compartmentalise the BZ media within a LM, which remains intact longer than the ferroin takes to oxidise, paves the way for future studies on BZ LM systems. Studying wave propagation in hexagonal arrays of BZ LMs, will provide a more natural arrangement for the LMs, in terms of spherical packing and also advantageous in terms of increasing the number of neighbours for each LM within an array. This will aim to establish whether the number of interface contacts affects the oscillating nature of the BZ media inside LMs. Different techniques for controlled initiation of waves will be analysed, such as using a hot Ag wire, varying light intensity (if using the light sensitive catalyst) and / or altering the chemical composition of the LM e.g. adding methanol or formaldehyde to the BZ media inside the LM [115] or tailoring the powder coating. In terms of tailoring the powder coating, it will be interesting to study the excitation dynamics in LMs made from BZ stock solutions and impregnating the powder coating with BZ catalyst, as well as analysing the suitability of other powder coatings with catalysed BZ solutions. It will also be interesting to explore methods for preparing the BZ reaction in-situ through LM merging [85, 116], to compare with the results reported here for BZ LMs prepared by encapsulating the already oscillating BZ solution. Further evidence of liquid–liquid communication between LMs, as assumed to be observed in the arrays reported above, will be sought through monitoring the transport of fluorescent particles through LM arrays. Diffusive coupling and excitation transfer has previously been observed in liquid based BZ systems. Other methods of monitoring the BZ reaction within LMs will be assessed, such as tuning the setup of arrays and taking electrical measurements of the encapsulated BZ solution. Future work will also study changing the chemical composition of the BZ media for example using a mixed 1,4-cyclohexanedione (CHD) / malonic acid variant of the reaction [117] or using protic ionic liquids [118]. The mixed CHD / malonic acid system reduced the induction periods compared to using CHD only, as well as reducing the gas evolution associated with the malonic acid system.

Numerical models of a light sensitive BZ medium encapsulated in geometric discs have demonstrated the feasibility of using this type of chemical system to implement polymorphic logic gates [119]. The presence/ absence of oxidation wave-fronts at a given point were interpreted as TRUE/FALSE Boolean values with computations occurring via the interactions of these wave-fronts. By changing the illumination on the chemical media, it was possible to program the outcomes of computation between XNOR and NOR gates [58]. Future studies will focus on implementing polymorphic logic gates with various arrangements of BZ LMs.

Conclusions

Using LM preparation methods has proved to be a promising means of encapsulating the BZ media within small droplets that have solid–liquid interfaces. This work reports the first fabrication of BZ solution droplets encapsulated in a powder coating, termed here as BZ LMs. The LMs are novel in comparison to other BZ encapsulation systems studied, such as BZ vesicles and catalyst loaded particles as the entire oscillating reaction is confined in a solid powder coating. The powder coating enables the LMs to be rolled and transferred onto different substrates without wetting the underlying surface. Therefore, the LMs could be moved at varying speeds to essentially create a stirred reactor vessel from the LMs. In the case of the experiments reported here, the LMs would be classed as unstirred reactors. Oxidation waves were visible through the coatings of the LMs, so the reaction could be monitored. The versatility of LMs, in terms of being able to tailor the encapsulated liquid and powder coating provide an attractive system for encapsulating an oscillating media for the purposes of chemical information transmission and the development of new unconventional computing devices.

Acknowledgements

This research was supported by the EPSRC with grant EP/P016677/1 “Computing with Liquid Marbles”.

Conflicts of interest

There are no conflicts to declare.

References

[1] Epstein I R and Xu B 2016 Reaction-diffusion processes at the nano- and microscales *Nat. Nanotechnol.* 11, 312-319

[2] Sun Y and Xia Y 2002 Shape-controlled synthesis of gold and silver nanoparticles *Science* 298, 2176–2179

[3] Sun Y, Mayers B T and Xia Y 2002 Template-engaged replacement reaction: A one-step approach to the large-scale synthesis of metal nanostructures with hollow interiors *Nano Lett.* 2, 481-485

[4] Kawamura R, Kakugo A, Shikinaka K, Osada Y and Gong J P 2008 Ring-shaped assembly of microtubules shows preferential counterclockwise motion *Biomacromolecules* 9, 2277-2282

[5] Yin Y, Rioux R M, Erdonmez C K, Hughes S, Somorjai G A and Alivisatos A P 2004 Formation of hollow nanocrystals through the nanoscale Kirkendall effect *Science* 304, 711–714

[6] Mattia E and Otto S 2015 Supramolecular systems chemistry *Nat. Nanotechnol.* 10, 111-119

[7] Mann S 2009 Self-assembly and transformation of hybrid nano-objects and nanostructures under equilibrium and non-equilibrium conditions *Nat. Mater.* 8, 781-792

[8] Epstein I R, Vanag V K, Balazs A C, Kuksenok O, Dayal P and Bhattacharya A 2012 Chemical oscillators in structured media *Accounts Chem. Res.* 45, 2160-2168

[9] Bánsági T, Vanag V K and Epstein I R 2011 Tomography of reaction-diffusion microemulsions reveals three-dimensional Turing patterns *Science* 331, 1309–1312

[10] Vanag V K and Epstein I R 2001 Inwardly rotating spiral waves in a reaction-diffusion system *Science* 294, 835–837

[11] Vanag V K and Epstein I R 2001 Pattern formation in a tunable medium: The Belousov-Zhabotinsky reaction in an aerosol OT microemulsion *Phys. Rev. Lett.* 87, 228301

[12] Totz J F, Engel H and Steinbock O 2015 Spatial confinement causes lifetime enhancement and expansion of vortex rings with positive filament tension *New J. Phys.* 17, 093043

[13] Belousov B P 1959 Periodically acting reaction and its mechanism *Compilation of Abstracts on Radiation Medicine*

[14] Zhabotinsky A 1964 Periodic processes of malonic acid oxidation in a liquid phase *Biofizika* 9, 11

[15] Kuhnert L 1986 A new optical photochemical memory device in a light-sensitive chemical active medium *Nature* 319, 393-394

[16] Kuhnert L, Agladze K I and Krinsky V I 1989 Image processing using light-sensitive chemical waves *Nature* 337, 244-247

[17] Kaminaga A, Vanag V K and Epstein I R 2006 A reaction–diffusion memory device *Angew. Chem. Int. Edit.* 45, 3087-3089

[18] Steinbock O, Kettunen P and Showalter K 1996 Chemical wave logic gates *J. Phys. Chem.* 100, 18970–18975

[19] Sielewiesiuk J and Górecki J 2001 Logical functions of a cross junction of excitable chemical media *J. Phys. Chem. A* 105, 8189–8195

[20] Steinbock O, Tóth Á and Showalter K 1995 Navigating complex labyrinths: Optimal paths from chemical waves *Science* 267, 868–871

[21] Rambidi N and Yakovenchuk D 2001 Chemical reaction-diffusion implementation of finding the shortest paths in a labyrinth *Phys. Rev. E* 63, 026607

[22] Adamatzky A and de Lacy Costello B 2002 Collision-free path planning in the Belousov-Zhabotinsky medium assisted by a cellular automaton *Naturwissenschaften* 89, 474–478

[23] Gorecki J, Gorecka J and Adamatzky A 2014 Information coding with frequency of oscillations in Belousov-Zhabotinsky encapsulated disks *Phys. Rev. E* 89, 042910

[24] Adamatzky A 2004 Collision-based computing in Belousov-Zhabotinsky medium *Chaos Solitons Fract.* 21, 1259–1264

[25] Yokoi H, Adamatzky A, de Lacy Costello B and Melhuish C 2004 Excitable chemical medium controller for a robotic hand: Closed-loop experiments *Int. J. Bifurcat. Chaos* 14, 3347–3354

[26] Vazquez-Otero A, Faigl J, Duro N and Dormido R 2014 Reaction-diffusion based computational model for autonomous mobile robot exploration of unknown environments *IJUC* 10, 295–316

[27] Igarashi Y and Gorecki J 2011 Chemical diodes built with controlled excitable media *IJUC* 7, 141–158

[28] Gorecki J, Gorecka J N and Igarashi Y 2009 Information processing with structured excitable medium *Nat. Comput.* 8, 473–492

[29] Stovold J and O'Keefe S 2012 Simulating neurons in reaction-diffusion chemistry *International Conference on Information Processing in Cells and Tissues* (Springer) pp 143–149

[30] Gentili P L, Horvath V, Vanag V K and Epstein I R 2012 Belousov-Zhabotinsky "chemical neuron" as a binary and fuzzy logic processor. *IJUC* 8, 177–192

[31] Takigawa-Imamura H and Motoike I N 2011 Dendritic gates for signal integration with excitability-dependent responsiveness *Neural Networks* 24, 1143–1152

[32] Gruenert G, Gizynski K, Escuela G, Ibrahim B, Gorecki J and Dittrich P 2015 Understanding networks of computing chemical droplet neurons based on information flow *Int. J. Neural Syst.* 25, 1450032

[33] Ke H, Tinsley M R, Steele A, Wang F and Showalter K 2014 Link weight evolution in a network of coupled chemical oscillators *Phys. Rev. E* 89, 052712

[34] Gentili P L, Giubila M S, Germani R and Heron B M 2018 Photochromic and luminescent compounds as artificial neuron models *Dyes Pigments* 156, 149 - 159

[35] Stovold J and O'Keefe S 2016 Reaction–diffusion chemistry implementation of associative memory neural network *Int. J. Parallel Emergent Distrib. Syst.* 32, 74-94

[36] Stovold J and O'Keefe S 2017 Associative memory in reaction-diffusion chemistry *Advances in Unconventional Computing* (Springer) pp 141–166

[37] Gorecki J, Yoshikawa K and Igarashi Y 2003 On chemical reactors that can count *J. Phys. Chem. A* 107, 1664–1669

[38] Yoshikawa K, Motoike I, Ichino T, Yamaguchi T, Igarashi Y, Gorecki J and Gorecka J N 2009 Basic information processing operations with pulses of excitation in a reaction-diffusion system *IJUC* 5, 3–37

[39] Escuela G, Gruenert G and Dittrich P 2014 Symbol representations and signal dynamics in evolving droplet computers *Nat. Comput.* 13, 247–256

[40] Gorecki J, Gizynski K, Guzowski J, Gorecka J, Garstecki P, Gruenert G and Dittrich P 2015 Chemical computing with reaction–diffusion processes *Phil. Trans. R. Soc. A* 373, 20140219

[41] Kramb R C, Buskohl P R, Dalton M J and Vaia R A 2015 Belousov–Zhabotinsky hydrogels: Relationship between hydrogel structure and mechanical response *Chem. Mater.* 27, 5782-5790

[42] Chang K M, de Planque M R and Zauner K P 2016 Fabricating millifluidic reaction-diffusion devices: Droplet-in-oil networks structured by laser cutting *Computational Intelligence (SSCI), 2016 IEEE Symposium Series on* (IEEE) pp 1–7

[43] Steinbock O and Müller S C 1998 Radius-dependent inhibition and activation of chemical oscillations in small droplets *J. Phys. Chem. A* 102, 6485-6490

[44] Gizynski K and Gorecki J 2017 Chemical memory with states coded in light controlled oscillations of interacting Belousov–Zhabotinsky droplets *Phys. Chem. Chem. Phys.* 19, 6519-6531

[45] Guzowski J, Gizynski K, Gorecki J and Garstecki P 2016 Microfluidic platform for reproducible self-assembly of chemically communicating droplet networks with predesigned number and type of the communicating compartments *Lab Chip* 16, 764-772

[46] Kitahata H, Aihara R, Magome N and Yoshikawa K 2002 Convective and periodic motion driven by a chemical wave *J. Chem. Phys.* 116, 5666-5672

[47] Kitahata H, Yoshinaga N, Nagai K H and Sumino Y 2012 Spontaneous motion of a Belousov–Zhabotinsky reaction droplet coupled with a spiral wave *Chem. Lett.* 41, 1052-1054

[48] Litschel T, Norton M M, Tserunyan V and Fraden S 2018 Engineering reaction-diffusion networks with properties of neural tissue *Lab Chip* 18, 714-722

[49] Suematsu N J, Mori Y, Amemiya T and Nakata S 2016 Oscillation of speed of a self-propelled Belousov–Zhabotinsky droplet *J. Phys. Chem. Lett.* 7, 3424-3428

[50] Stricker L 2017 Numerical simulation of artificial microswimmers driven by marangoni flow *J. Comput. Phys.* 347, 467 - 489

[51] Torbensen K, Rossi F, Ristori S and Abou-Hassan A 2017 Chemical communication and dynamics of droplet emulsions in networks of Belousov–Zhabotinsky micro-oscillators produced by microfluidics *Lab Chip* 17, 1179–1189

[52] Torbensen K, Ristori S, Rossi F and Abou-Hassan A 2017 Tuning the chemical communication of oscillating microdroplets by means of membrane composition *J. Phys. Chem. C* 121, 13256–13264

[53] Tamate R, Ueki T, Shibayama M and Yoshida R 2017 Effect of substrate concentrations on the aggregation behavior and dynamic oscillatory properties of self-oscillating block copolymers *Phys. Chem. Chem. Phys.* 19, 20627-20634

[54] Tamate R, Ueki T, Shibayama M and Yoshida R 2017 Autonomous unimer-vesicle oscillation by totally synthetic diblock copolymers: Effect of block length and polymer concentration on spati-temporal structures *Soft Matter* 13, 4559-4568

[55] Hu Y and Pérez-Mercader J 2016 Microfluidic fabrication of polymersomes enclosing an active Belousov–Zhabotinsky (BZ) reaction: Effect on their stability of solute concentrations in the external media *Colloid. Surface. B* 146, 406 - 414

[56] Stockmann T J, Noël J M, Ristori S, Combellas C, Abou-Hassan A, Rossi F and Kanoufi F 2015 Scanning electrochemical microscopy of Belousov–Zhabotinsky reaction: How confined oscillations reveal short lived radicals and auto-catalytic species *Anal. Chem.* 87, 9621-9630

[57] Pereira de Souza T and Perez-Mercader J 2014 Entrapment in giant polymersomes of an inorganic oscillatory chemical reaction and resulting chemo-mechanical coupling *Chem. Commun.* 50, 8970-8973

[58] Wang A, Gold J, Tompkins N, Heymann M, Harrington K and Fraden S Configurable NOR gate arrays from Belousov–Zhabotinsky micro-droplets

[59] Rossi F, Ristori S, Rustici M, Marchettini N and Tiezzi E 2008 Dynamics of pattern formation in biomimetic systems *J. Theor. Biol.* 255, 404 - 412

[60] Vanag V K and Epstein I R 2002 Packet waves in a reaction-diffusion system *Phys. Rev. Lett.* 88, 088303

[61] Vanag V K and Epstein I R 2003 Dash waves in a reaction-diffusion system *Phys. Rev. Lett.* 90, 098301

[62] McIlwaine R, Vanag V K and Epstein I R 2009 Temperature control of pattern formation in the $[Ru(bpy)_3]^{2+}$-catalyzed BZ–AOT system *Phys. Chem. Chem. Phys.* 11, 1581-1587

[63] Gong Y and Christini D J 2003 Antispiral waves in reaction-diffusion systems *Phys. Rev. Lett.* 90, 088302

[64] Cherkashin A A and Vanag V K 2017 Self-organization induced by self-assembly in microheterogeneous reaction-diffusion system *J. Phys. Chem. B* 121, 2127-2131

[65] Maselko J and Showalter K 1989 Chemical waves on spherical surfaces *Nature* 339, 609-611

[66] Taylor A F, Tinsley M R and Showalter K 2015 Insights into collective cell behaviour from populations of coupled chemical oscillators *Phys. Chem. Chem. Phys.* 17, 20047-20055

[67] Nishiyama N and Eto K 1994 Experimental study on three chemical oscillators coupled with time delay *J. Chem. Phys.* 100, 6977-6978

[68] Nishiyama N 1995 Experimental observation of dynamical behaviors of four, five and six oscillators in rings and nine oscillators in a branched network *Physica D* 80, 181 - 185

[69] Aihara R and Yoshikawa K 2001 Size-dependent switching of the spatiotemporal structure between a traveling wave and global rhythm *J. Phys. Chem. A* 105, 8445-8448

[70] Kuze M, Kitahata H, Steinbock O and Nakata S 2018 Distinguishing the dynamic fingerprints of two- and three-dimensional chemical waves in microbeads *J. Phys. Chem. A* 122, 1967-1971

[71] Totz J F, Rode J, Tinsley M R, Showalter K and Engel H 2018 Spiral wave chimera states in large populations of coupled chemical oscillators *Nat. Phys.* 14, 282-285

[72] King P H, Jones G, Morgan H, de Planque M R and Zauner K P 2014 Interdroplet bilayer arrays in millifluidic droplet traps from 3d-printed moulds *Lab Chip* 14, 722–729

[73] King P H, Abraham C H, Zauner K P and de Planque M R 2015 Excitability modulation of oscillating media in 3D-printed structures *Artif. Life* 21, 225–233

[74] Aussillous P and Quéré D 2001 Liquid marbles *Nature* 411, 924–927

[75] Ireland P M, Thomas C A, Lobel B T, Webber G B, Fujii S and Wanless E J 2018 An electrostatic method for manufacturing liquid marbles and particle-stabilized aggregates *Frontiers in Chemistry* 6, 280

[76] Bormashenko E, Pogreb R, Musin A, Balter R, Whyman G and Aurbach D 2010 Interfacial and conductive properties of liquid marbles coated with carbon black *Powder Technol.* 203, 529 - 533

[77] McHale G 2009 All solids, including teflon, are hydrophilic (to some extent), but some have roughness induced hydrophobic tendencies *Langmuir* 25, 7185-7187

[78] Bormashenko E 2017 Liquid marbles, elastic nonstick droplets: From minireactors to self-propulsion *Langmuir* 33, 663–669

[79] Bormashenko E 2012 New insights into liquid marbles *Soft Matter* 8, 11018–11021

[80] Fujii S, Yusa S I and Nakamura Y 2016 Stimuli-Responsive Liquid Marbles: Controlling Structure, Shape, Stability, and Motion *Adv. Funct. Mater.* 26, 7206–7223

[81] McHale G and Newton M I 2015 Liquid marbles: Topical context within soft matter and recent progress *Soft Matter* 11, 2530–2546

[82] Ooi C H and Nguyen N T 2015 Manipulation of liquid marbles *Microfluid. Nanofluid.* 19, 483–495

[83] Rycheckỳ O, Majerská M, Král V, Štěpánek F and Čejková J 2017 Spheroid cultivation of HT-29 carcinoma cell line in liquid marbles *Chem. Pap.* 71, 1055–1063

[84] Draper T C, Fullarton C, Phillips N, de Lacy Costello B P J and Adamatzky A 2018 Liquid marble actuator for microfluidic logic systems *Sci. Rep.-UK* 8, 14153

[85] Draper T C, Fullarton C, Phillips N, de Lacy Costello B P and Adamatzky A 2017 Liquid marble interaction gate for collision-based computing *Mater. Today* 20, 561–568

[86] Aussillous P and Quéré D 2006 Properties of liquid marbles *Proc. R. Soc. A Math. Phys. Eng. Sci.* 462, 973–999

[87] Bormashenko E 2011 Liquid marbles: Properties and applications *Curr. Opin. Colloid In.* 16, 266–271

[88] Bormashenko E and Bormashenko Y 2011 Non-stick droplet surgery with a superhydrophobic scalpel *Langmuir* 27, 3266–3270

[89] Bormashenko E, Pogreb R, Balter R, Aharoni H, Bormashenko Y, Grynyov R, Mashkevych L, Aurbach D and Gendelman O 2015 Elastic properties of liquid marbles *Colloid Polym. Sci.* 293, 2157–2164

[90] Bhosale P S, Panchagnula M V and Stretz H A 2008 Mechanically robust nanoparticle stabilized transparent liquid marbles *Appl. Phys. Lett.* 93, 034109

[91] Zhao Y, Fang J, Wang H, Wang X and Lin T 2010 Magnetic liquid marbles: Manipulation of liquid droplets using highly hydrophobic Fe_3O_4 nanoparticles *Adv. Mater.* 22, 707–710

[92] Dandan M and Erbil H Y 2009 Evaporation rate of graphite liquid marbles: Comparison with water droplets *Langmuir* 25, 8362-8367

[93] Dupin D, Thompson K L and Armes S P 2011 Preparation of stimulus-responsive liquid marbles using a polyacid-stabilised polystyrene latex *Soft Matter* 7, 6797-6800

[94] Xue Y, Wang H, Zhao Y, Dai L, Feng L, Wang X and Lin T 2010 Magnetic liquid marbles: A “precise” miniature reactor *Adv. Mater.* 22, 4814-4818

[95] Gao L and McCarthy T J 2007 Ionic liquid marbles *Langmuir* 23, 10445-10447

[96] Tian J, Arbatan T, Li X and Shen W 2010 Liquid marble for gas sensing *Chem. Commun.* 46, 4734-4736

[97] Vadivelu R K, Kamble H, Munaz A and Nguyen N T 2017 Liquid marbles as bioreactors for the study of three-dimensional cell interactions *Biomed. Microdevices* 19, 31

[98] Arbatan T, Li L, Tian J and Shen W 2012 Liquid marbles as micro-bioreactors for rapid blood typing *Adv. Healthc. Mater.* 1, 80-83

[99] Fujii S, Sawada S, Nakayama S, Kappl M, Ueno K, Shitajima K, Butt H J and Nakamura Y 2016 Pressure-sensitive adhesive powder *Mater. Horiz.* 3, 47-52

[100] Sheng Y, Sun G, Wu J, Ma G and Ngai T 2015 Silica-based liquid marbles as microreactors for the silver mirror reaction *Angew. Chem. Int. Edit.* 54, 7012-7017

[101] Field R J and Winfree A T 1979 Travelling waves of chemical activity in the Zaikin-Zhabotinskii-Winfree reagent *J. Chem. Educ.* 56, 754

[102] Fullarton C, Draper T C, Phillips N, Mayne R, de Lacy Costello B P J and Adamatzky A 2018 Evaporation, lifetime, and robustness studies of liquid marbles for collision-based computing *Langmuir* 34, 2573-2580

[103] Rendos A, Alsharif N, Kim B L and Brown K A 2017 Elasticity and failure of liquid marbles: influence of particle coating and marble volume *Soft Matter* 13, 8903-8909

[104] Avrămescu R E, Ghica M V, Dinu-Pîrvu C, Udeanu D I and Popa L 2018 Liquid marbles: From industrial to medical applications *Molecules* 23, 1120

[105] Nguyen T H, Hapgood K and Shen W 2010 Observation of the liquid marble morphology using confocal microscopy *Chem. Eng. J.* 162, 396 - 405

[106] Bormashenko E, Pogreb R, Whyman G and Musin A 2009 Surface tension of liquid marbles *Colloid. Surface. A* 351, 78 - 82

[107] Sreejith K R, Ooi C H, Dao D V and Nguyen N T 2018 Evaporation dynamics of liquid marbles at elevated temperatures *RSC Adv.* 8, 15436-15443

[108] F Taylor A, R Johnson B and K Scott S 1999 Scroll waves in the Belousov–Zhabotinsky reaction: exploitation of O_2-effect on the ferroin-catalysed system *Phys. Chem. Chem. Phys.* 1, 807-811

[109] Tian J, Arbatan T, Li X and Shen W 2010 Porous liquid marble shell offers possibilities for gas detection and gas reactions *Chem. Eng. J.* 165, 347 - 353

[110] Onel L, Wittmann M, Pelle K, Noszticzius Z and Sciascia L 2007 The source of the carbon monoxide in the classical Belousov–Zhabotinsky reaction *J. Phys. Chem. A* 111, 7805-7812

[111] Miike H, Sakurai T, Nomura A and Müller S C 2015 Chemically driven convection in the Belousov–Zhabotinsky reaction–Evolutionary pattern dynamics *Forma* 30, 33 - 53

[112] De Lacy Costello B, Jahan I, Ahearn M, Holley J, Bull L and Adamatzky A 2013 Initiation of waves in BZ encapsulated vesicles using light - Towards design of computing architectures *IJUC* 9, 311–326

[113] Tinsley M R, Taylor A F, Huang Z and Showalter K 2009 Emergence of collective behavior in groups of excitable catalyst-loaded particles: Spatiotemporal dynamical quorum sensing *Phys. Rev. Lett.* 102, 158301

[114] Totz J F, Snari R, Yengi D, Tinsley M R, Engel H and Showalter K 2015 Phase-lag synchronization in networks of coupled chemical oscillators *Phys. Rev. E* 92, 022819

[115] van Roekel H W H, Rosier B J H M, Meijer L H H, Hilbers P A J, Markvoort A J, Huck W T S and de Greef T F A 2015 Programmable chemical reaction networks: Emulating regulatory functions in living cells using a bottom-up approach *Chem. Soc. Rev.* 44, 7465-7483

[116] Liu Z, Fu X, Binks B P and Shum H C 2016 Coalescence of electrically charged liquid marbles *Soft Matter* 13, 119–124

[117] Chang K M, de Planque M R R and Zauner K P 2018 Towards functional droplet architectures: A Belousov-Zhabotinsky medium for networks *Sci. Rep.-UK* 8, 12656

[118] Ueki T, Watanabe M and Yoshida R 2012 Belousov–Zhabotinsky reaction in protic ionic liquids *Angew. Chem. Int. Edit.* 51, 11991-11994

[119] Adamatzky A, De Lacy Costello B, Dittrich P, Gorecki J and Zauner K P 2014 On logical universality of Belousov-Zhabotinsky vesicles *Int. J. Gen. Syst.* 43, 757–769